Physica D 492 (2026) 135209

Contents lists available at ScienceDirect

Physica D

journal homepage: www.elsevier.com/locate/physd

Oscillatory cell membrane potentials and ion channel protein transcription: a biophysical model

Josu Egea-Carro [a], Salvador Mafe [a,b], Javier Cervera [a,*]

[a] Departament de Termodinamica, Universitat de Valencia, Dr. Moliner, 50, Burjassot, 46100, Valencia, Spain
[b] Allen Discovery Center, Tufts University, 200 Boston Avenue, Medford, 02155, Massachussets, United States of America

ARTICLE INFO

Keywords:
Cell membrane potential
Oscillations
Ion channel
Protein transcription
Biophysical model

ABSTRACT

The interplay between genetic and bioelectric networks is of significance in Biophysics because voltage-gated ion channels are involved in multitude of development, regeneration, and tumorigenesis processes. We have developed a model that shows the rich biophysical dynamics that can occur at the individual cell scale. In particular, we have theoretically characterized monostable and bistable stationary as well as oscillatory cell membrane potentials on the basis of a system of differential equations that couple together two generic families of ion channels. The model incorporates a minimal number of biologically-plausible assumptions that are independent from specific microscopic details. The electrical rhythms found provide an oscillatory feedback between bioelectrical and transcriptional signals that can be experimentally modulated by external actions on specific ion channels.

1. Introduction

Bioelectrochemistry is central to development and regeneration because the cell membrane potential, defined as the (negative) potential difference established between the cell cytoplasm and the external microenvironment [1–3], is a master regulator for biochemical processes in non-excitable cells. Although the cell potential is not a transcription factor itself, it influences downstream transcription processes, e.g. by regulating the local concentration of signaling ions and molecules such as calcium [2–5]. The significant role of bioelectric signals has also been demonstrated in the maintenance of organism morphology and cancer progression [1–6]. Because cell potentials are modulated by the ion channel proteins inserted in the cell membrane [1,7], it is important to understand their underlying biophysical dynamics. In order to motivate our mathematical analysis, Figs. 1a-d consider four biological systems where our modeling should be of qualitative interest. Two examples of the coupling between bioelectrical and biochemical signals are the electrogenetic circuit [8] of Fig. 1a and the cell potential influence on the timing of pluripotency genes [9] shown in the model of Fig. 1b. In both cases, the concerted action of two counteracting voltage-gated channels regulates the membrane potential values that control the inside calcium levels required for crucial downstream biochemical processes [8,9]. Fig. 1c concerns an excitable cell model where the inside cell calcium level is also coupled to the gene expression of two ion channels [10]. Fig. 1d corresponds to the case of Ca^{2+} flux-coupled gene regulation in *Escherichia Coli*. The depolarization of the cell potential changes the inside calcium ion concentration, producing downward changes in the expression of different proteins [11].

In general, electric potential variations at the cellular level can be transduced downstream because bioelectric signals regulate the electrodiffusion not only of calcium ions, but also of other charged signalling molecules, as discussed in Ref [2]. and references therein. This experimental integration between bioelectric signals and biochemical messengers should first be understood in terms of simple models.

Models that describe the feedback between cell potentials and protein transcription can provide new insights on both morphogenesis and tumorigenesis [2,3,12–15]. In previous studies, we have explored theoretically the interplay between genetic and bioelectric networks by focusing on *multicellular aggregates* [3,16]. Here, we aim at describing the rich dynamics and bifurcation phenomena that can occur at the *single-cell scale* because of the coupling between cell membrane potentials and channel protein transcription. This coupling offers a useful complementary view to the traditional description that tends to emphasize biochemical effects only [7], thus ignoring important *bioelectrochemical* phenomena. Here, we consider a minimal model for the coupling between ionic currents and a gene regulatory network.

Note that oscillatory cell membrane potentials are central to the cell cycle [17], pancreatic islets [18], glioma cells [19], bacterial communities [20], and synchronization phenomena [21] where different channel actions provoke the oscillation of the cell membrane potential. Bistability and oscillatory coupling between bioelectrical (cell potential) and biochemical (intracellular calcium concentration) signals are

* Corresponding author.
E-mail address: javier.cervera@uv.es (J. Cervera).

https://doi.org/10.1016/j.physd.2026.135209
Received 11 September 2025; Received in revised form 10 March 2026; Accepted 25 March 2026
Available online 2 April 2026

also characteristic of excitation waves in multicellular pancreatic islets [22]. Also, cell potentials and cytoplasmic calcium levels are interrelated in *Xenopus* embryogenesis [23] where particular instructive windows are experimentally observed. In this context, different mechanisms underlying the influence of bioelectricity in development have been described.

Clearly, the above examples suggest that ion channels, cell potentials, and signaling ions levels can be coupled in bistable and oscillatory memories. The main contribution of this study is to determine what basic properties are relevant to the understanding of bistable and oscillatory dynamics at the individual cell level. To this end, we will analyze the phase space region where the cell undergoes self-sustained oscillations as a result of the feedback between the regulation of the mRNAs that codify the proteins inserted in the membrane as voltage-gated ion channels. In addition, we will compare this scenario with that where mRNAs are not regulated by the cell potential so that a bistable region instead of an oscillatory one is observed.

2. Biophysical model equations

It is an experimental fact that bioelectric signals regulate the voltage-gated channels that govern the transport of ions and signalling charged molecules which are instructive for downstream processes [2–5]. In general, the cell potential V can be considered as a readout of the cell bioelectrical activity. For instance, proliferative cells tend to show abnormally depolarized potentials (low values of $|V|$), contrary to the case of quiescent differentiated cells [2,5]. Thus, the cell electric potential should be incorporated in the kinetic equations that regulate channel protein expression. We have proposed the simplified coupling scheme of Fig. 2, which is based on the experimentally plausible assumptions discussed previously [3]. Although a diversity of protein ion channels are inserted in the membrane, a limited number of specific channels experimentally determine the cell potential [2,3,5,19–25], as shown in the experimental systems of Fig. 1. Thus, we have introduced two generic voltage-gated ion channels, the polarizing (*pol*) channel promoting a high absolute value of the cell potential $|V|$ and the depolarizing (*dep*) channel aiming at decreasing $|V|$ [3]. Note that because $V < 0$, the $|V|$ terms could be replaced with $-V$ terms here.

The cell potential $V < 0$ is obtained from the zero current equation [3], $I_{dep} + I_{pol} = 0$, where $I_{dep} = G_{dep}(V - E_{dep})/\{1 + \exp[-z(V - V_{th,dep})/V_T]\}$ and $I_{pol} = G_{pol}(V - E_{pol})/\{1 + \exp[z(V - V_{th,pol})/V_T]\}$ are the electrical currents through the *dep* and *pol* channels that connect the external microenvironment with the cell cytoplasm (Fig. 2). In the I_{dep} and I_{pol} equations, C is the cell capacitance, z gives the number of effective charges for channel gating, and $V_{th,dep}$ and $V_{th,pol}$ are the threshold potentials. The thermal potential $V_T = RT/F = 27$ mV, where R is the gas constant, $T = 310$ K is the temperature, and F is the Faraday constant [3]. Note that V is regulated by the *dep* and *pol* conductance values G_{dep} and G_{pol} that attempt to establish the equilibrium depolarized and polarized potentials $E_{dep} = 0$ mV and $E_{pol} = -60$ mV. If the cell is in contact with a sufficiently large microenvironment, the extracellular ionic concentrations do not change. Also, the number of ions transported across the membrane to establish a given value of V is usually small compared with the total number of ions in the cell. This

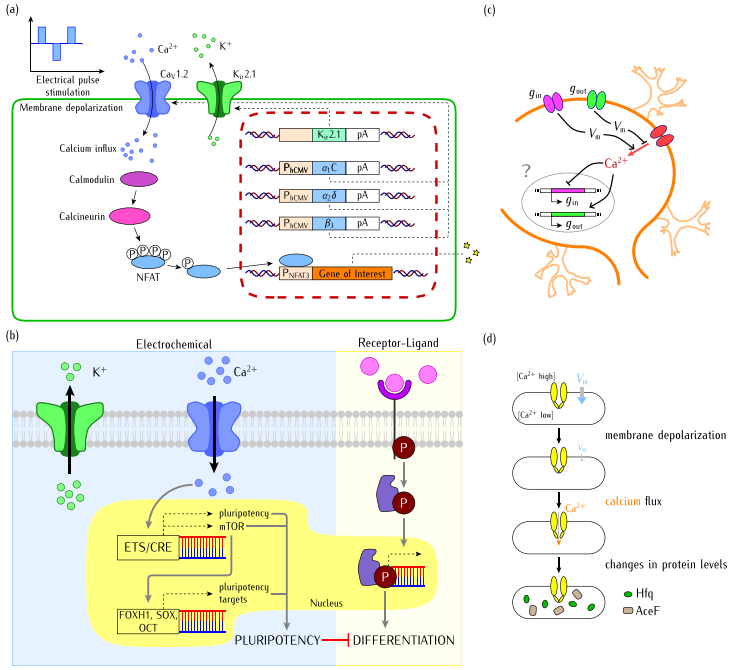

Fig. 1. a) Transcriptional control of mammalian cells by membrane depolarization shows the coupling between bioelectrical and biochemical signals. In the electrogenetic circuit, an inward-rectifying potassium (Kir) channel sets initially the potential of human embryonic kidney (HEK-293T) cells. External pulses provoke the depolarization that opens the voltage-gated calcium channel (Cav). The increase in the calcium level yields downstream processes (activation of the calmodulin/calcineurin pathway, dephosphorylation of the nuclear factor of activated T cells (NFAT), and the NFAT-sensitive promoter) towards the target transgene expression. Figure adapted from Krawczyk *et al.*, Science doi:10.1126/science.aau7187, AAAS [8]. (b) Membrane potential (left) and receptor-ligand (right) signaling in the onset of embryonic differentiation. Potassium channels set the polarized cell potential, which keeps voltage-gated calcium channels closed, thus avoiding the high calcium levels required for downstream processes to pluripotency. While gene expression is also mediated by intracellular signal transducers and biochemical pathways essential to the expression of differentiation factors, bioelectricity may influence also the timing of pluripotency genes. Figure adapted from Sempou *et at.*, Nature Communications, doi:10.1038/s41467-022-34363-w, Springer-Nature [9]. (c) Scheme of a neuron potential model regulated by inward and an outward channel conductances whose counteracting actions control the Ca^{2+} influx. The calcium ion level downward modulates channel transcription. Figure adapted from O'Leary et al., PNAS, doi: 10.1073/pnas.1309966110, pnas.org., [10]. (d) Calcium ion flux-coupled gene regulation in *Escherichia Coli*. The cell potential can be depolarized by the action of different channel conductances, with the concomitant changes in the inside calcium level that downward regulate the expression of proteins. Figure adapted from Jones and Larkin, Bioelectricity, doi: 10.1089/bioe.2021.0013, Mary Ann Liebert, Inc. [11].

fact, together with the continuous action of the ion pumps [1], results in approximately constant intracellular concentrations and equilibrium potentials.

The membrane potential regulates the inside levels of second messengers of concentration S_k that can act downstream on the transcription of the channels. For instance, calcium levels can have different effects on distinct channel proteins expressions via the binding to distinct intermediate proteins, which can eventually impact on the membrane potential via the different protein channel conductances, as biologically motivated in the examples of Figs. 1c and 1d and theoretically explained previously [3]. Thus, a crucial assumption of the model is that the protein transcription rates $r_{m,k}$ are functions of the cell potential V because the concentrations S_{dep} and S_{pol} of instructive signaling ions or molecules depend on V. The equations that relate these magnitudes are given in Fig. 3. The regulation of the transcription rates by the potential, which is experimentally suggested in Fig. 1, provides the feedback between the genetic and the bioelectric signals. Here, we are concerned with the *relatively slow* membrane potential changes observed in non-excitable cells where the effective channel conductance is expected to increase linearly with the protein concentration p_k *in the cytoplasm* only for low protein concentrations, but to reach a saturation (*maximum*) value because of the unavoidable kinetic limitations at high enough p_k. These limitations arise from the finite rates for trafficking to and insertion in the cell membrane, the effective membrane area that is available for insertion, and the channel operation life in the membrane. In this complex experimental context, the phenomenological Hill kinetics equation $G_k = G_k^\circ p_k/(p_{0,k} + p_k)$ provides a useful first approximation because it suggests that the effective channel conductance cannot increase indefinitely with the *bulk protein concentration* p_k, but should achieve a maximum value G_k° for high enough concentrations $p_k \gg p_{0,k}$ with respect to a characteristic saturation conductance $p_{0,k} = 80$, where the above kinetic limitations dictate the inserted channel proteins available for ionic conduction.

The genetic network of Fig. 2 follows the biochemical central dogma principle that states the flow of information from DNA to mRNA (transcription) to protein (translation). Note however that, in our extended coupling scheme, the expression of the ion channels that regulate the cell potential V are in turn influenced by V (Fig. 3). For instance, if the conductance ratio G_{dep}/G_{pol} becomes too high, V deviates from the physiological polarized potential E_{pol} by taking abnormally depolarized potentials close to E_{dep}. This perturbation triggers a counteracting compensation because of the resulting increase in the rate of $r_{m,pol}(V)$ of Fig. 3 [3].

Table 1
Value of the parameters that remain constant in the simulations.

Magnitude	Value
E_{pol}	−60 mV
E_{dep}	0 mV
$V_{th,pol}$	$-V_T = -27$ mV
$V_{th,dep}$	$-V_T = -27$ mV
z_{pol}	2
z_{dep}	2
G_{pol}°/G_{ref}	1.0
G_{dep}°/G_{ref}	1.0
$r_{m,dep}^\circ$	1.5 min^{-1}
$d_{m,dep}$	0.05 min^{-1}
$r_{p,pol}$	1.5 min^{-1}
$d_{p,pol}$	0.05 min^{-1}
$r_{p,dep}$	1.5 min^{-1}
$d_{p,dep}$	0.05 min^{-1}
$p_{pol,0}/p_{ref}$	80
$p_{dep,0}/p_{ref}$	80

The coupling model of Figs. 2 and 3 can be extended further by incorporating additional equations relevant to other problems in embryogenesis, regeneration, and tumorigenesis [2,3,5,12,17,21], thus offering a phenomenological feedback mechanism between the biochemical and bioelectric networks in each particular case. In principle, the counteracting mechanism of Fig. 3 can allow oscillatory cell potentials without an outside pacemaker.

3. Model parameters

The model rate constants of Fig. 2 should be considered only as effective values because transcription, translation, and degradation depend on multiple factors characterized by different intermediate steps. Table 1 shows typical rates estimated as 0.1-5 min^{-1} for transcription and 0.1-2 min^{-1} for the case of translation [3,14,15,21]. Degradation rate constants should be in the range 0.001-0.1 min^{-1} for characteristic times between minutes and hours [3,14,15,21]. These values show that genetic processes are comparatively slow with respect to cell electrical times, which can be estimated as C/G_{ref}, where G_{ref} is a reference conductance that allows to present the results in terms of relative values. Indeed, for the cell capacitance $C = 10$ - 100 pF and the reference channel conductance $G_{ref} = 0.1$ nS, the electrical times are in the 0.1 - 1 s range [3]. Here, we have considered different exploratory simulations

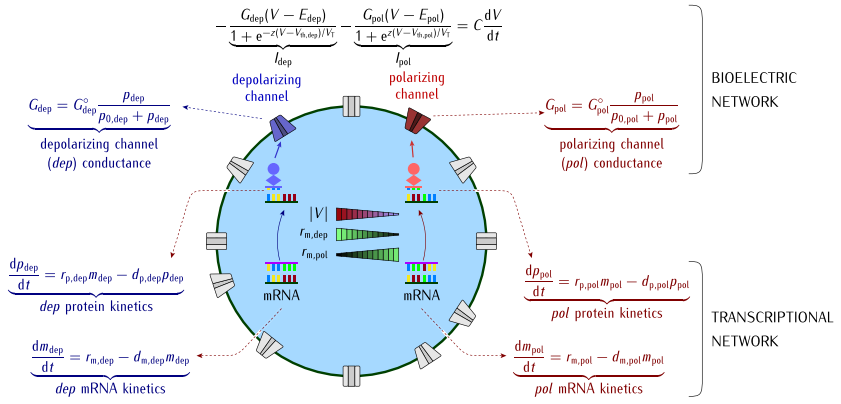

Fig. 2. The bioelectrical and transcriptional feedback for two generic channel proteins that regulate the polarized (*pol*) and depolarized (*dep*) cell states, as described in References [3,21]. The protein transcription and translation are described by kinetic equations for the mRNA concentrations m_{dep} and m_{pol} and the protein concentrations p_{dep} and p_{pol}, respectively, which are relative values that depend on the biosystem considered. Here, molecular diffusion within the cell is ignored because it should be relatively fast compared with the underlying genetic processes. The mRNA transcription ($r_{m,k}$) and protein translation ($r_{p,k}$) rate constants, together with their respective degradation rates ($d_{m,k}$ and $d_{p,k}$), with k = pol, dep, are effective values for the multiple kinetic steps that may be involved. Note the dependence of the cell potential-regulated transcription rates on the absolute value of the cell potential $|V|$.

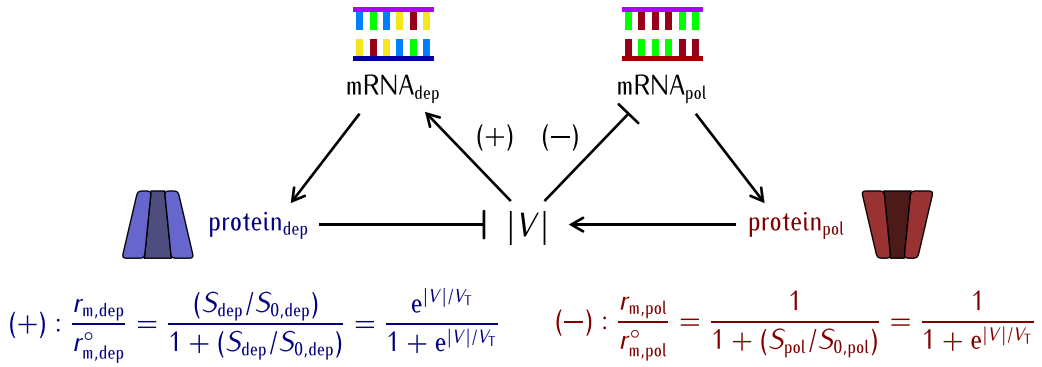

Fig. 3. The feedback between the cell potential $V < 0$ and the mRNA transcription rate $r_{m,k}(V)$ regulates the channel protein concentration, where $r_{m,k}(V=0) = r^{\circ}_{m,k}/2$ (k = pol, dep). The potential regulation is positive (+) for the *dep* channel protein and negative (-) for the *pol* channel protein. Here, S_k (k = pol, dep) is the concentration of an ion or molecule that is instructive for the downstream channel transcription and $S_{0,k}$ is a reference concentration, as described in Reference [3]. The coupling between biochemical and bioelectric processes occurs because the cell potential V modulates the channel protein concentration p_k that eventually gives the conductance G_k and, in turn, the conductance G_k modulates the potential V, as shown in Fig. 2.

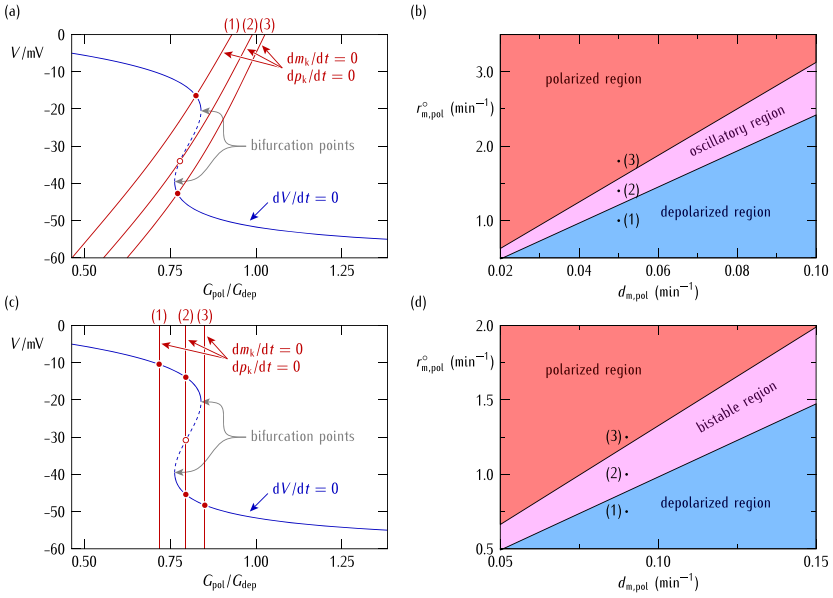

Fig. 4. The fixed points of the dynamical system of Fig. 2 are obtained by the intersection between the bioelectrical ($dV/dt = 0$) curve and the genetic ($dm_k/dt = 0$, $dm_k/dt = 0$, k = pol, dep) curve (Fig. 4a and 4c). The $dV/dt = 0$ curve shows two saddle-node bifurcation points that delimit the stable (continuum lines) and unstable (dashed line) solutions. The intersection of the genetic curve in stable and unstable points of the bioelectrical curve results in the phase-space (Fig. 4b and 4d). Fig. 4a and 4b correspond to the potential regulated transcriptional rate, with the parameters $d_k = 0.05$ min^{-1} and the cases $r^{\circ}_{m,k} = 1.0$ min^{-1} (1), 1.4 min^{-1} (2), and 1.8 min^{-1} (3), k = pol, dep. Figs. 4c and 4d correspond to the non-regulated transcriptional rate with $d_{m,k} = 0.09$ min^{-1} and the cases $r^{\circ}_{m,k} = 0.75$ min^{-1} (1), 1.00 min^{-1} (2) and 1.25 min^{-1} (3). The other parameters employed are shown in Table 1.
The labels (1) - (3) indicate the cell state initial points whose trajectories are analyzed later.

for the system of coupled differential equations (Fig. 2) by introducing a range of typical parameters (Table 1). A full justification of their biological plausibility, together with other explorations of the parameter space, have been given previously [3,21]. In addition, mathematical and numerical details concerning the simulation algorithm can be found in [3] and references therein.

4. Results and discussion

4.1. Fixed points and phase space

We assume that the only magnitudes that change in the *pol* and *dep* channels are the conductances G_{pol} and G_{dep} through the variation of their expressions following the respective transcription-translation networks. The fixed points of the system are obtained by imposing that all time derivatives of Fig. 2 are zero. Thus, the equation $C dV/dt = -I_{pol} - I_{dep} = 0$ gives the steady-state solutions of the potential as a function of the ratio G_{pol}/G_{dep}, as shown in Figs. 4a and 4c. Monostable regions for the cell potential are obtained for low (depolarized solution) and high (polarized solution) values of G_{pol}/G_{dep}. There are two saddle-node bifurcation points where either a couple of (stable polarized-unstable) or (stable depolarized-unstable) fixed points are created/annihilated [26]. These critical points delimit the bistable region where two stable solutions (continuum lines) coexists with an unstable solution (dashed line) in Figs. 4a and 4c. The unstable state represents an equilibrium between the *pol* and the *dep* channels whereas, in the stable states, one of the channel types eventually dominates, depending on the initial conditions .

By imposing that the time derivatives of m_k and p_k, k = pol, dep, are zero, we obtain a second relation between the steady state values of V and G_{pol}/G_{dep} that the fixed points must obey. Therefore, the fixed points of the dynamical systems correspond to the intersection between

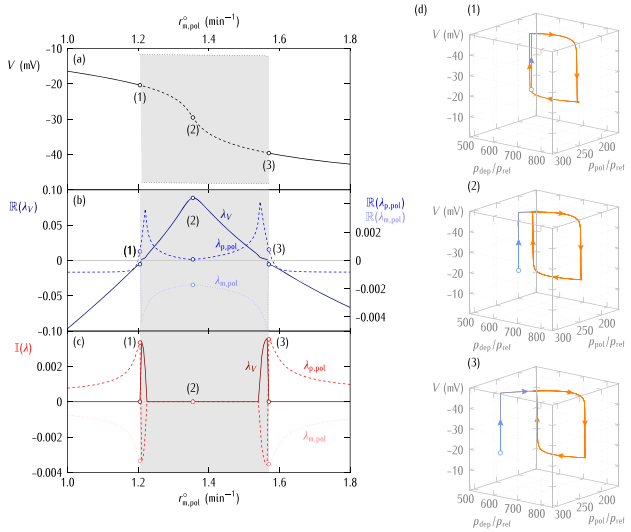

Fig. 5. (a) Bifurcation diagram for $d_{\mathrm{m,pol}} = 0.05\ \mathrm{min}^{-1}$ and the parameters of Table 1 when the mRNA transcription rates are regulated by the cell potential V. The stable solutions of V are indicated by a continuum line that turns unstable at the oscillating region (gray zone), which is indicated by a dashed line. The height of the gray zone is limited by the maximum and minimum potential attained in the oscillation. (b) Real part of the eigenvalues of V, p_{pol} and m_{pol}. (c) Imaginary part of the eigenvalues of V, p_{pol} and m_{pol}. (d) Trajectory $(p_{\mathrm{pol}}, p_{\mathrm{dep}}, V)$ of points (1)-(3) of Fig. 5a-c.

the bioelectrical ($\mathrm{d}V/\mathrm{d}t = 0$) and the genetic ($\mathrm{d}p_{\mathrm{k}}/\mathrm{d}t = 0$, $\mathrm{d}m_{\mathrm{k}}/\mathrm{d}t = 0$) steady-state curves. In the case of Fig. 4a, the regulation of the transcriptional rate with the potential implies that these two curves intersect in either a unique stable or unstable solution of the potential. The intersection in the stable solutions results in the polarized and depolarized solutions, and the intersection in the unstable solution leads to self-sustained oscillations, thus giving the phase-space of Fig. 4b. By contrast, when the transcriptional rate is not regulated by the potential (Fig. 4c), the bioelectrical and genetic curves can intersect in either one stable solution (monostable polarized or depolarized) or in three solutions (two stable and one unstable), resulting in the phase space of Fig. 4d.

Note finally that, with a different set of parameters, the case of regulated transcriptional rate can also lead to a bistability instead of an oscillatory regime if the bioelectrical and genetic curves intersect not only in the unstable potential solution but also in the stable potential solutions [27].

Taking together, Fig. 4 should be useful to qualitatively understand how the inside concentration of a signaling ion can couple bioelectrical to genetic networks (Fig. 2) through the cell potential regulation of the transcriptional rates (Fig. 3), as experimentally shown for the calcium entry following cell depolarization (Fig. 1). Clearly, the model of Figs. 2 and 3 suggest how the control of the polarized and depolarized cell states can be crucial for the cell biophysics, thus allowing to guide external actions on membrane potentials.

4.2. Eigenvalues

Mathematically, we can obtain more information relevant to the fundamental nature of the cell states by calculating the eigenvalues of the Jacobian from the dynamical system of equations at Figs. 2 and 3 [26]. Fig. 5a shows the bifurcation diagram for $d_{\mathrm{m,pol}} = 0.05\ \mathrm{min}^{-1}$ for the case of cell potential-regulated mRNA transcription rates, but this time as a function of $r^{\circ}_{\mathrm{m,pol}}$. Figs. 5b and c show the real and imaginary parts of the eigenvalues λ_V of the potential V and the protein and mRNA concentrations p_{pol} and m_{pol} of the *pol* channel, respectively. The eigenvalues of protein and mRNA concentration of the *dep* channel take constant real values over the whole $r^{\circ}_{\mathrm{m,pol}}$ interval considered and have not been represented. The eigenvalues have been calculated at the predicted steady-state values, given by the continuum and dashed lines of Fig. 5a for the case of the potential.

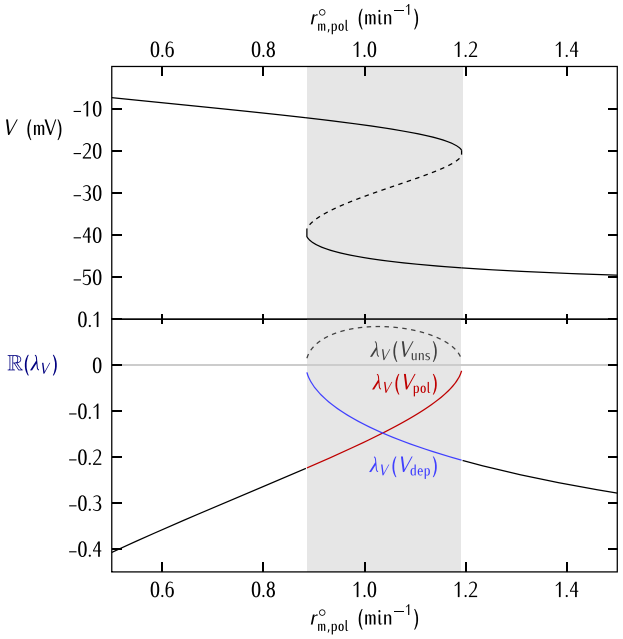

Fig. 6. (a) Bifurcation diagram for $d_{\mathrm{m,pol}} = 0.09\ \mathrm{min}^{-1}$ and the parameters of Table 1 in the case of unregulated mRNA rates. At low and high values of $r^{\circ}_{\mathrm{m,pol}}$ there is only one steady-state stable solution for the potential (continuum line). At intermediate values, however, the cell enters into the bistable region characterized by two stable solutions (polarized and depolarized, continuum line) and one unstable solution (dashed line). (b) Eigenvalue of V calculated at the stable solution for the monostable zones and all three solutions for the bistable zone. The stable solutions are characterized by a negative value of the (real) eigenvalue whereas the unstable solution is characterized by a positive value (dashed line).

The stable and oscillatory regions coincide with the zones where the real part $\mathbb{R}(\lambda_V)$ is negative and positive, respectively. The value of $\mathbb{R}(\lambda_V)$ would approximately indicate where the solution of the potential is stable ($\mathbb{R}(\lambda_V) < 0$) and unstable ($\mathbb{R}(\lambda_V) > 0$). Note also the narrow regions

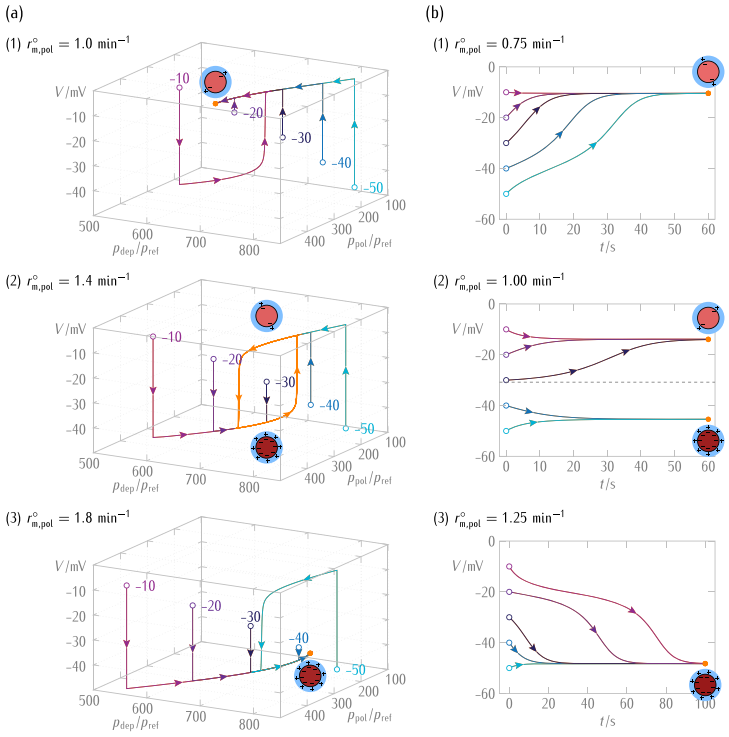

Fig. 7. (a) Phase space evolution of the (V, p_{pol}, p_{dep}) initial points (1)-(3) in Fig. 4a and 4b (cell potential-regulated transcription rates). (b) Evolution of V for the phase space points (1)-(3) of Fig. 4c and 4d (the case of unregulated transcription rates).

in the transitions between the stable and the oscillatory regimes where the imaginary part of λ_V is non-zero and those of $\lambda_{p,pol}$ and $\lambda_{m,pol}$ undergo abrupt changes (Figs. 5b and 5c). This may reflect the fact that the transition between the stable solutions (continuum lines) and the oscillatory solutions (dashed lines) is abrupt in the sense that the radius of the limit cycle of the oscillatory regions does not increase smoothly but undergoes a discontinuous jump, in agreement with the comparatively fast cell bioelectrical responses [2–5]. However, no qualitative changes in the evolution of the cell is observed when the trajectories of the three cases considered here ((1) and (3) in the narrow region, (2) outside the narrow region) are calculated (Fig. 5d). In all three cases, a limit cycle is observed.

Fig. 6a reconsiders the bifurcation diagram for the case of unregulated mRNA transcription rates with $d_{m,pol} = 0.09$ min^{-1} using $r^{\circ}_{m,pol}$ as a parameter and the values of Table 1 for the magnitudes involved. Because the transcription rate is not regulated by the potential, the $dV/dt = 0$ curves in Fig. 6a and Fig. 4c are qualitatively similar. The eigenvalue of the potential λ_V (Fig. 6b) at the steady-state solutions of Fig. 6a shows that the negative real values of λ_V coincide with the stable solutions while the positive values coincide with the unstable solution. Taking together, Figs. 5 and 6 provide a complementary mathematical description of the different bioelectrical and transcriptional cell states that can be obtained with the model, thus offering a more rigorous view of the biochemical problem.

4.3. Trajectories

To better visualize the evolution of the cell state in the regulated case, Fig. 7a shows the evolution of (p_{pol}, p_{dep}, V) from the different phase space initial states of Fig. 4a-b: depolarized (1), oscillatory (2), and polarized (3). To obtain the initial state of the cell, we first set the potential V. Then, the values of m_{pol}, p_{pol} (G_{pol}), m_{dep} and p_{dep} (G_{dep}) are obtained by determining the transcription rates $r^{\circ}_{m,pol}$ and $r^{\circ}_{m,dep}$ at this potential from Fig. 3, and then using the equations of Fig. 2 with zero time derivatives for mRNA and protein concentrations.

In the first part of the (p_{pol}, p_{dep}, V) evolution, the potential relaxes to the bioelectrical stable point determined by G_{dep} and G_{pol} because, initially, the sum of currents $I_{pol} + I_{dep} \neq 0$. In this bioelectrically-driven process, the transcription-translation magnitudes (p_{pol} and p_{dep} in the figure) remain practically constant as their transcriptional time is of the order of 1 h, as dictated by the inverse of the rate and degradation constants, and hence much longer than the bioelectric time which is of the order of 1 s. Because the values of these transcription-translation magnitudes have been set in accordance with the initial potential, the change of the cell potential implies that p_{pol} and p_{dep}, as well as m_{pol} and m_{dep}, are no longer in equilibrium. Therefore, a second, transcriptionally driven process starts where p_{pol} and p_{dep} vary while the potential change is much smaller and slave to the change of the transcription-translation variables. Finally, the cell reaches either a stable point ($r^{\circ}_{m,pol} = 1.0$ min^{-1} and 1.8 min^{-1}) or enters a limit cycle ($r^{\circ}_{m,pol} = 1.4$ min^{-1}). In some cases, another pair of processes (first bioelectrically-driven, then transcriptionally-driven) take place before reaching the stable point. These are the cases for the initial potentials -10 mV when $r^{\circ}_{m,pol} = 1.0$ min^{-1} and -50 mV when $r^{\circ}_{m,pol} = 1.8$ min^{-1} The limit cycle ($r^{\circ}_{m,pol} = 1.4$ min^{-1}) is formed by two bielectrically-driven (V changes and p_{pol} and p_{dep} are practically constant) and two transcriptionally-driven (V is practically constant and p_{pol} and p_{dep} change) processes that alternate.

Fig. 7b shows the evolution of the cell potential V with time for unregulated transcription rates in the cases (1) to (3) of Fig. 4c-d. Now the transcription and translation variables are constant and the relaxation time is a factor 10 - 100 lower than in the regulated case (Fig. 7a) because only V changes and thus its evolution is dictated by the bioelectrical characteristic time $\tau_{bioelec} = C/G_{ref} = 1$ s. When the cell is in a monostable region, the potential evolves until reaching the steady state solution (depolarized cell for $r^{\circ}_{m,pol} = 0.75$ min^{-1} and polarized cell for

$r^{\circ}_{m,pol} = 1.25\ min^{-1}$). In the bistable region, however, the final potential depends on whether the initial value of V is in the region of the depolarized or the polarized solution. These two regions are divided by the unstable potential (marked by a dashed line in Fig. 7b). In this way, Figs. 7a and 7b offer qualitative explanations for the different experimental time regimes characteristic of the external bioelectrical actions and the comparatively slow downstream biochemical outcomes [2–5,8,9].

5. Conclusions

Ion channels are central to the bi-stability and oscillatory phenomena experimentally observed in many cell regulatory processes , as shown by current pharmacological and optogenetic techniques which allow direct manipulation of membrane potential and hypothesis testing (Refs [15–24].). Models describing the interplay between genetic and bioelectric networks are of great significance because voltage-gated ion channels are involved in multitude of development, regeneration, and tumorigenesis processes [2–5]. Thus, theoretical approaches that integrate genetic and electric concepts can suggest new experimental opportunities (Fig. 1).

Here, we have focused on the rich dynamics and bifurcation phenomena that can occur at the individual cell scale. In particular, we have theoretically described the role of stationary and oscillatory cell membrane potentials on the basis of a system of differential equations that couple together two generic families of ion channels. For completeness, the unregulated case where there is no feedback between the bioelectrical and transcriptional networks has also been considered and significant differences with respect to the case of cell potential-regulated mRNA transcription rates have been found, as suggested by Fig. 1. In the unregulated case, a bistable region separating the depolarized and polarized regions is obtained instead of self-sustained oscillations.

A limitation of the results concerns our ignoring of the role of endoplasmic reticulum (ER) in intracellular calcium levels [28–30]. As to experimental observations on calcium oscillatory and spiking phenomena, it has been shown that the coupling between the cell potential and intracellular calcium can lead to bistable and oscillatory phenomena in the excitation waves of pancreatic islets, where the time traces of potentials and calcium concentrations are clearly coupled [22]. Also, the bioelectric activity in *Xenopus* embryogenesis is shown to be modulated by the interplay between the cell potential and the intracellular calcium level [23] where hyperpolarization and depolarization processes induce dynamic calcium changes at different developmental stages. These experimental results clearly suggest that ion channels, cell potentials, and signaling ions levels are coupled together in oscillatory and bi-stable memories, in qualitative agreement with the model predictions.

We believe that a theoretical description of the bioelectrical and transcriptional coupling can be useful to qualitatively guide future experimental studies. Note that bioelectrochemical oscillations expand across a range of temporal scales in biology [2,3,17–21]. In our case, the oscillatory phenomena arise from the coupling between the cell potentials and biochemical networks of two counteracting families of channel proteins. This simple model, which incorporates a minimal number of biologically-plausible assumptions, can now be extended to specific experimental cases. In conclusion, we have shown how the electrical rhythms that provide an oscillatory feedback between bioelectrical and transcriptional signals can be experimentally explored by particular external actions on specific ion channels.

CRediT authorship contribution statement

Josu Egea-Carro: Writing – review & editing, Validation, Software, Methodology, Investigation; **Salvador Mafe:** Writing – original draft, Supervision, Methodology, Funding acquisition, Conceptualization; **Javier Cervera :** Writing – review & editing, Visualization, Validation, Software, Project administration, Funding acquisition, Formal analysis.

Data availability

No data was used for the research described in the article.

Declaration of competing interest

The authors declare that they have no known competing financial interests or personal relationships that could have appeared to influence the work reported in this paper.

Acknowledgements

We acknowledge the support from the *Ministerio de Ciencia e Innovación* (Spain) and the European Regional Development Funds (FEDER), project PID2022-139953NB-I00.

References

[1] B. Hille, Ion Channel of Excitable Membranes, Sinauer Associates, Sunderland, Massachusetts, Sunderland, Massachusetts, 2001.
[2] M. Levin, Bioelectric signaling: reprogrammable circuits underlying embryogenesis, regeneration, and cancer, Cell 184 (2021) 1971–1989. https://doi.org/10.1016/j.cell.2021.02.034
[3] J. Cervera, M. Levin, S. Mafe, Bioelectricity of non-excitable cells and multicellular pattern memories: biophysical modeling, Phys. Rep. Rev. Sect. Phys. Lett. 1004 (2023) 1–31. https://doi.org/10.1016/j.physrep.2022.12.003
[4] E. Bates, Ion Channels in Development and Cancer, in: R. Schekman (Ed.), Annual Review of Cell and Developmental Biology, VOL 31, 31 of *Annual Review of Cell and Developmental Biology*, Annual Reviews, 2015, pp. 231–247. https://doi.org/10.1146/annurev-cellbio-100814-125338
[5] M. Yang, W.J. Brackenbury, Membrane potential and cancer progression, Frontiers Physiol. 4 (2013). https://doi.org/10.3389/fphys.2013.00185
[6] J. Krueger, J. Bohrmann, Bioelectric patterning during oogenesis: stage-specific distribution of membrane potentials, intracellular ph and ion-transport mechanisms in Drosophila ovarian follicles, BMC Dev. Biol. 15 (2015) 1. https://doi.org/10.1186/s12861-015-0051-3
[7] B. Alberts, A. Johnson, J. Lewis, M. Raff, K. Roberts, P. Walter, Molecular Biology of the Cell, Garland Science, New York, New York, 2002.
[8] K. Krawczyk, S. Xue, P. Buchmann, G. Charpin-El-Hamri, P. Saxena, M.-D. Hussherr, J. Shao, H. Ye, M. Xie, M. Fussenegger, Electrogenetic cellular insulin release for real-time glycemic control in type 1 diabetic mice, Science 368 (2020) 993–1001. https://doi.org/10.1126/science.aau7187
[9] E. Sempou, V. Kostiuk, J. Zhu, M.C. Guerra, L. Tyan, W. Hwang, E. Camacho-Aguilar, M.J. Caplan, D. Zenisek, A. Warmflash, N.D.L. Owens, M.K. Khokha, Membrane potential drives the exit from pluripotency and cell fate commitment via calcium and mTOR, Nature Commun. 13 (2022) 6681. https://doi.org/10.1038/s41467-022-34363-w
[10] T. O'Leary, A.H. Williams, J.S. Caplan, E. Marder, Correlations in ion channel expression emerge from homeostatic tuning rules, Proc. Natl. Acad. Sci. 110 (2013) E2645–E2654. https://doi.org/10.1073/pnas.1309966110
[11] J.M. Jones, J.W. Larkin, Toward Bacterial Bioelectric Signal Transduction, Bioelectricity 3 (2021) 116–119. PMID: 34476386. https://doi.org/10.1089/bioe.2021.0013
[12] V.P. Pai, X.M. Lemire, J.-F. Pare, G. Lin, Y. Chen, M. Levin, Endogenous Gradients of Resting Potential Instructively Pattern Embryonic Neural Tissue via Notch Signaling and Regulation of Proliferation, J. Neurosci. 35 (2015) 4366–4385. https://doi.org/10.1523/JNEUROSCI.1877-14.2015
[13] E. Levine, P. McHale, H. Levine, Small regulatory RNAs may sharpen spatial expression patterns, PLOS Comput. Biol. 3 (2007) 2356–2365. https://doi.org/10.1371/journal.pcbi.0030233
[14] V.P. Zhdanov, Kinetic models of gene expression including non-coding RNAs, Phys. Rep. Rev. Sect. Phys. Lett. 500 (2011) 1–42. https://doi.org/10.1016/j.physrep.2010.12.002
[15] V.P. Zhdanov, Three generic bistable scenarios of the interplay of voltage pulses and gene expression in neurons, Neural Networks 44 (2013) 51–63. https://doi.org/10.1016/j.neunet.2013.02.004
[16] J. Cervera, A. Pietak, M. Levin, S. Mafe, Bioelectrical coupling in multicellular domains regulated by gap junctions: a conceptual approach, Bioelectrochemistry 123 (2018) 45–61. https://doi.org/10.1016/j.bioelechem.2018.04.013
[17] V.R. Rao, M. Perez-Neut, S. Kaja, S. Gentile, Voltage-Gated Ion Channels in Cancer Cell Proliferation, Cancers 7 (2015) 849–875. https://doi.org/10.3390/cancers7020813
[18] T.H. Hraha, M.J. Westacott, M. Pozzoli, A.M. Notary, P.M. McClatchey, R.K.P. Benninger, Phase Transitions in the Multi-cellular Regulatory Behavior of Pancreatic Islet Excitability, PLOS Comput. Biol. 10 (2014) e1003819. https://doi.org/10.1371/journal.pcbi.1003819
[19] P.R.F. Rocha, P. Schlett, L. Schneider, M. Droege, V. Mailaender, H.L. Gomes, P.W.M. Blom, D.M. de Leeuw, Low frequency electric current noise in glioma cell populations, J. Mater. Chem. B 3 (2015) 5035–5039. https://doi.org/10.1039/c5tb00144g
[20] A. Prindle, J. Liu, M. Asally, S. Ly, J. Garcia-Ojalvo, G.M. Sueel, Ion channels enable electrical communication in bacterial communities, Nature 527 (2015) 59–63. https://doi.org/10.1038/nature15709

[21] J. Cervera, J. Antonio Manzanares, S. Mafe, M. Levin, Synchronization of Bioelectric Oscillations in Networks of Nonexcitable Cells: from single-cell to multicellular states, J. Phys. Chem. B 123 (18) (2019) 3924–3934. https://doi.org/10.1021/acs.jpcb.9b01717

[22] O.V. Aslanidi, O.A. Mornev, O. Skyggebjerg, P. Arkhammar, O. Thastrup, M.P. Sørensen, P.L. Christiansen, K. Conradsen, A.C. Scott, Excitation wave propagation as a possible mechanism for signal transmission in pancreatic islets of Langerhans, Biophys. J. 80 (2001) 1195–1209. https://doi.org/10.1016/S0006-3495(01)76096-1

[23] P. McMillen, R. Novak, M. Levin, Toward Decoding Bioelectric Events in Xenopus Embryogenesis: new methodology for tracking interplay between calcium and resting potentials in vivo, J. Mol. Biol. 432 (2) (2020) 605–620. https://doi.org/10.1016/j.jmb.2019.10.029

[24] V.P. Pai, A. Pietak, V. Willocq, B. Ye, N.-Q. Shi, M. Levin, HCN2 rescues brain defects by enforcing endogenous voltage pre-patterns, Nature Commun. 9 (2018) 998. https://doi.org/10.1038/s41467-018-03334-5

[25] F. Durant, J. Morokuma, C. Fields, K. Williams, D.S. Adams, M. Levin, Long-Term, Stochastic Editing of Regenerative Anatomy via Targeting Endogenous Bioelectric Gradients, Biophys. J. 112 (10) (2017) 2231–2243. https://doi.org/10.1016/j.bpj.2017.04.011

[26] S.H. Strogatz, Nonlinear Dynamics and Chaos, CRC Press, Boca Raton, Boca Raton, 2018.

[27] J. Cervera, S. Meseguer, S. Mafe, The interplay between genetic and bioelectrical signaling permits a spatial regionalisation of membrane potentials in model multicellular ensembles., Sci. Rep. 6 (2016) 35201. https://doi.org/10.1038/srep35201

[28] J. Humeau, J.M. B.-S. Pedro, I. Vitale, L. Nuñez, C. Villalobos, G. Kroemer, L. Senovilla, Calcium signaling and cell cycle: progression or death, Cell Calcium 70 (2018) 3–15. https://doi.org/10.1016/j.ceca.2017.07.006

[29] L. Catacuzzeno, B. Fioretti, F. Franciolini, A theoretical study on the role of Ca^{2+}-activated K^{+} channels in the regulation of hormone-induced Ca^{2+} oscillations and their synchronization in adjacent cells, J. Theor. Biol. 309 (2012) 103–112. https://doi.org/10.1016/j.jtbi.2012.05.009

[30] G.R. Monteith, N. Prevarskaya, S.J. Roberts-Thomson, The calcium-cancer signalling nexus, Nature Rev. Cancer (2017) 367–380. https://doi.org/10.1038/ncr.2017.18